Broadband Optically Transparent Absorber and Multi-Band Stealth Based on Organic Metasurface

Chuwen Lan[1†], Yutong Gao[1†], Zehua Gao[1*], Hongye Wang[1], Ke Bi[2*], Ming Lei[3*], and Guoan Zhao[4]

[1]*School of Information and Communication Engineering, Beijing Laboratory of Advanced Information Networks; Beijing Key Laboratory of Network System Architecture and Convergence, Beijing University of Posts and Telecommunications, Beijing 100876, China*
[2]*State Key Laboratory of Information Photonics and Optical Communications, School of Science, Beijing University of Posts and Telecommunications, Beijing 100876, China*
[3]*School of Integrated Circuits, Beijing University of Posts and Telecommunications, Beijing 100876, China*
[4]*Network Education College of Beijing University of Posts and Telecommunications, Beijing 100876, China*

(Received 8 February 2025; accepted manuscript online 16 April 2025)

Optically transparent microwave absorbers and multi-band stealth have extensive potential applications in military defense and wireless communication fields, and thus have attracted considerable attention. So far, most related work is based on inorganic transparent conductive metasurfaces. In this paper, we proposed and experimentally demonstrated a flexible, broadband and optically transparent microwave absorber using an organic metasurface. The metasurface absorber is composed of a sandwich structure, in which electric resonances and magnetic resonances are induced resulting in broadband absorption. A spraying process was developed to prepare this metasurface absorber. Both simulations and experiment show that this metasurface has broadband microwave absorption and good optical transparency. We further found that by using a multi-layer structure, visible, radar, and infrared stealth (multi-band stealth) can be achieved simultaneously. With the advantages of excellent foldability and low cost, the proposed metasurfaces may have applications in military and wireless communication fields.

DOI: 10.1088/0256-307X/42/5/056303 CSTR: 32039.14.0256-307X.42.5.056303

1. Introduction. Absorbers represent a class of structures or materials capable of absorbing incident electromagnetic waves while minimizing reflected waves as much as possible.[1–4] Absorbers play a crucial role in stealth technology, communication, and electromagnetic shielding or protection.[5–13] Traditionally, absorbers are made of materials based on various mechanisms like conduction loss, magnetic loss or dielectric loss. However, the inherent properties of traditional materials impose limitations on the performance. Over the past few years, metamaterials or metasurface absorbers have drawn extensive attention and have become a research hotspot. Electromagnetic metamaterials or metasurfaces are artificial structures composed of periodic or non-periodic sub-wavelength resonators. Interestingly, their electromagnetic properties do not stem from the constituent materials themselves, but rather from the resonators' configurations, dimensions and arrangements.[14] Through reasonable designs, a large number of different metamaterial absorbers have been investigated and reported.[15–18]

On the other hand, optically transparent microwave absorbers have attracted much attention due to their applications in some scenarios, like fairings, aircraft canopies and multi-band stealth.[19,20] However, the realization of optically transparent absorbers is quite a challenging task because it is difficult for most materials to obtain microwave absorption and optical transparency simultaneously. Fortunately, metamaterial absorbers offer a promising solution to this problem. In the past years, exciting results have been reported, such as broadband absorption,[21–32] ultra-thin thickness,[33–36] and even multi-band stealth.[37–46] Up to now, most of the optically transparent microwave metamaterial absorbers are based on inorganic conductive films, like indium tin oxide (ITO).[21–28,36,40,42,43] Despite their numerous advantages, the application of inorganic oxide-based structures in some specific fields is still limited, especially in achieving irregular surfaces, low-cost, and foldable absorbers.

Here, a flexible, broadband and optically transparent microwave absorber using an organic metasurface is proposed and experimentally demonstrated. The metasurface absorber is composed of a sandwich structure. The upper and lower layers are periodic resonators and reflective layers composed of organic conductive films, and the middle layer is air. A spraying process was developed to prepare this metasurface absorber. Both simulations and experiment show that this metasurface has broadband microwave absorption and optical transparency. We further

[†]These authors contributed equally to this work.
[*]Corresponding author. Email: gaozehua@bupt.edu.cn; bike@bupt.edu.cn; mlei@bupt.edu.cn
© 2025 Chinese Physical Society and IOP Publishing Ltd. All rights, including for text and data mining, AI training, and similar technologies, are reserved.

found that by using a multi-layer structure, visible stealth, microwave absorption and infrared stealth can be achieved simultaneously.

2. Concept and Design. The concept of the designed multi-band stealth can be seen in Fig. 1. The multi-band stealth consists of an infrared low emissivity metasurface, a broadband optically transparent absorber and an optical camouflage substrate. When the target that requires to be protected is covered with multi-band stealth, radar and infrared cameras cannot detect it due to low radar reflectivity and low infrared emissions. Since both the absorber and the low-emissivity metasurface are optically transparent, optical camouflage is simultaneously achieved. In this multi-band camouflage scheme, optically transparent radar absorber is the key.

The proposed absorber based on an organic metasurface is shown in Fig. 2(a). It consists of a sandwich structure. The upper and lower layers are periodic resonators and reflective layers composed of organic conductive films, and the middle layer is air. We use treated PEDOT:PSS films for the organic conductive films due to their high conductivity and stable performance, as well as low cost.[47] In this structure, the reflective layer on the bottom of the unit cell is a continuous organic conductive film [Fig. 2(b)], designed to prevent most electromagnetic waves from passing through the structure. The upper metasurface is composed of periodic concentric split-ring patterns, separated by air layers. By appropriately designing the patterns of the metasurface and the thickness of the air layer, impedance matching is expected to be achieved, ultimately enabling broadband microwave absorption. Owing to the exceptional optical transparency of PEDOT:PSS films, it can be utilized to achieve optically transparent microwave absorption. The thickness and sheet resistance of the organic conductive film are about 300 nm and 35–40 Ω/sq. The polyethylene terephthalate (PET) with a dielectric constant of 3.0 and a loss tangent of 0.006 is used as a supporting layer of the organic conductive films. The final dimensional parameters are shown in Fig. 2(b), where $w = 18$ mm, $d_{\text{air}} = 3.3$ mm, $d_{\text{PET}} = 0.175$ mm, $r = 8.5$ mm, $g_1 = 0.5$ mm, $g_0 = 0.5$ mm, $r_{\text{d}} = 1.5$ mm.

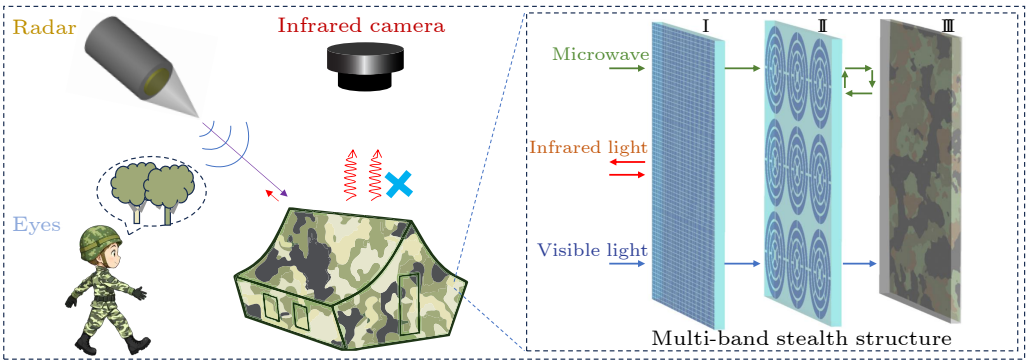

Fig. 1. Concept of the designed multi-band stealth and broadband optically transparent absorber based on an organic metasurfaces. Ⅰ, Ⅱ, Ⅲ are low emissivity metasurface, optically transparent absorber and optical camouflage substrate, respectively.

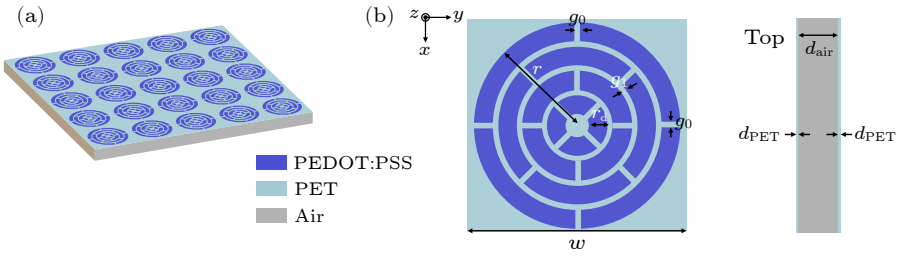

Fig. 2. Schematic of the organic metasurface absorber. (a) Perspective view. (b) Top view and side view of unit cell.

3. Simulation and Analysis. To investigate the performance of the absorbing structure, we conducted numerical simulations. In simulations, the electric field (E) and the magnetic field (H) are oriented along the x- and y-directions, respectively, and the propagation direction of electromagnetic waves (k) is along the z direction [as shown in Fig. 2(b)]. By using the finite integration method, we obtain the S_{11} (reflection coefficient) and S_{21} (transmission coefficient) of the structure. Then, the absorptivity of the metasurface structure can be calculated as $A(\omega) = 1 - R(\omega) - T(\omega)$, where the reflectivity $R(\omega)$ is equal to $|S_{11}|^2$, and the transmissivity $T(\omega)$ is equal to $|S_{21}|^2$. The simulation results of the reflectivity, transmissivity, and absorptivity of the metasurface absorber are shown in Fig. 3. Since a continuous organic conductive film is employed as the bottom layer, this structure effectively isolates the majority of electromagnetic waves, resulting in a low transmissivity. In addition, the reflection coefficient is very low above 8.0 GHz. From the absorptivity curve, it can be observed that the absorber exhibits an absorptivity

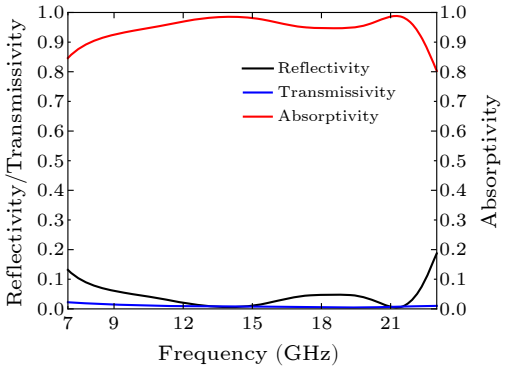

Fig. 3. The simulated transmissivity, reflectivity and absorptivity of organic metasurface absorber.

exceeding 90% from 8.0 GHz to 22.4 GHz, indicating that this absorber has excellent broadband absorption capability.

To explore the underlying mechanism of the broadband absorber, we investigate the corresponding equivalent impedance. The relationship between the reflection coefficient (R) of the metasurface and its equivalent impedance (Z_L) is expressed as $R = \frac{Z_L - Z_0}{Z_L + Z_0} = \frac{Z-1}{Z+1}$, where Z_0 represents the impedance of free space, and $Z = Z_L/Z_0$ denotes the normalized equivalent impedance. Consequently, as the normalized equivalent impedance of the metasurface approaches 1, the reflectivity diminishes towards 0, enabling good wave absorption. The transfer matrix function of metasurface structures is [48]

$$T = \begin{pmatrix} \cos(nkd) & -\frac{z}{k}\sin(nkd) \\ \frac{k}{z}\sin(nkd) & \cos(nkd) \end{pmatrix} \tag{1}$$

in which d, k, n, and z represent the thickness of the equivalent material, wave vector, refractive index, and equivalent impedance respectively. Moreover, the S parameters and transmission matrix T of metasurface structures satisfy [48]

$$S_{11} = S_{22} = \frac{\mathrm{i}}{2}\left(\frac{1}{z} - z\right)\sin(nkd), \tag{2}$$

$$S_{12} = S_{21} = \frac{1}{\cos(nkd) - \frac{\mathrm{i}}{2}\left(z + \frac{1}{z}\right)\sin(nkd)}. \tag{3}$$

Combining the above two equations, the equivalent impedance of the metasurface can be retrieved using the S_{11} and S_{21} parameters, which is given by [48,49]

$$z = \sqrt{\frac{(1+S_{11})^2 - S_{21}^2}{(1-S_{11})^2 - S_{21}^2}}. \tag{4}$$

The calculated normalized equivalent impedance of the metasurface is shown in Fig. 4. Notably, within the bandwidth ranging from 8.0 to 22.4 GHz, where the absorptivity of the metasurface absorber surpasses 90%, the real part of the normalized equivalent impedance approximates to 1, while the imaginary part is around zero. At this point, the equivalent impedance Z_L of the metasurface is almost identical to the vacuum impedance Z_0, achieving impedance matching. Therefore, it exhibits excellent microwave absorption capability.

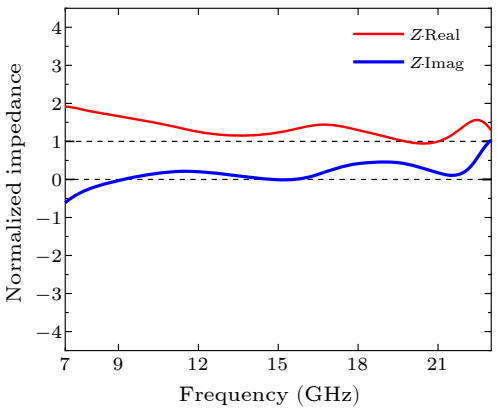

Fig. 4. Calculated normalized impedance for overall input impedance of organic metasurface absorber.

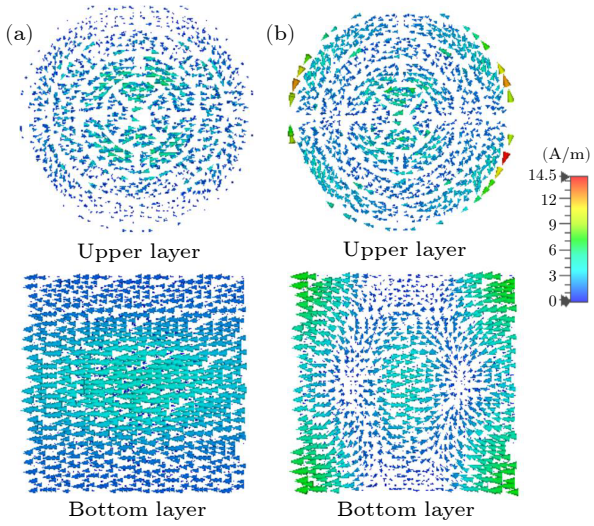

Fig. 5. Surface current distributions at the upper and lower layers of organic metasurface absorber at (a) 14.04 GHz and (b) 21.3 GHz.

Simulations of surface current distributions for the upper and lower layers are conducted to analyze the electromagnetic mechanism. The frequencies (14.04 GHz, 21.3 GHz) where the two absorption peaks occur are investigated (Fig. 5). It can be seen that enhanced surface currents appear at the upper layer for two frequencies indicating electric resonances are induced. As for the bottom layer, opposite enhanced surface currents are observed. These opposite enhanced surface currents, in cooperation with currents on the upper layer, form current loops, and eventually result in magnetic resonances. That means the absorption is the result of both electric resonances and magnetic resonances.

4. Fabrication. In order to fabricate this microwave absorber, a simple and low-cost spraying process was developed. The corresponding fabrication process can be seen in Fig. 6. Firstly, a PET film with a thickness of 0.175 mm is cut into the required area and then placed on a heating plate. The temperature of the heating plate is set at 120 ℃. Secondly, a metal mask fabricated by traditional metal etching process is placed on the PET substrate [Fig. 6(b)]. Thirdly, PEDOT:PSS based solution is loaded into a spray gun for spraying.

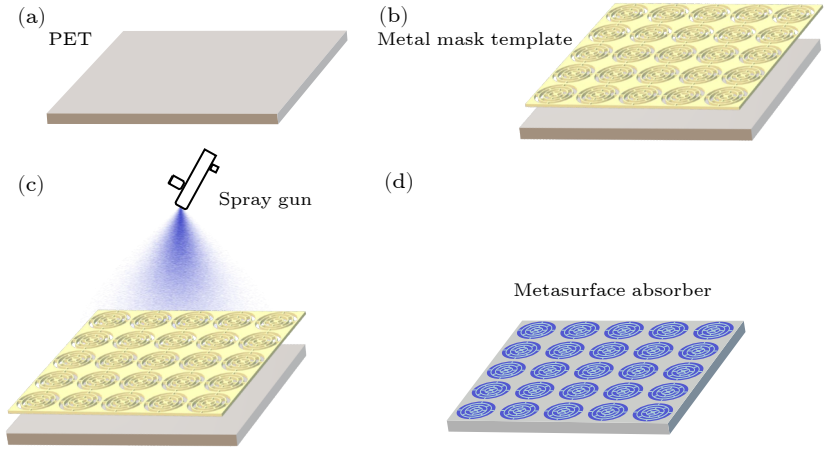

Fig. 6. Fabrication process of organic metasurface absorber.

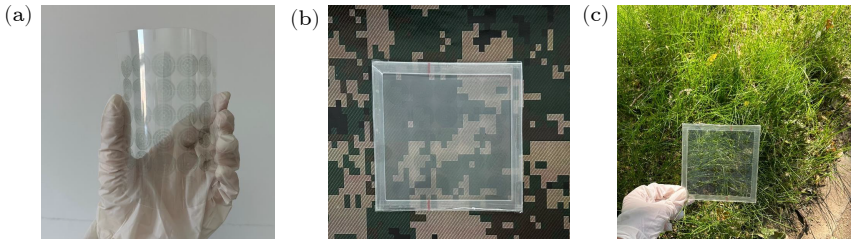

Fig. 7. Photographs of fabricated metasurface (a) under the bending state, (b) placed on a camouflage pattern, (c) in the open air.

The thickness of the PEDOT:PSS films can be controlled by spraying time and air pressure. PEDOT:PSS based metasurface is fabricated by a heating process. The fabricated PEDOT:PSS based metasurface and PEDOT:PSS substrate are then separated by a PMMA frame, thus a microwave absorber is obtained.

In the preparation, the PET substrate requires corona treatment, which can enhance the adhesion between the substrate and PEDOT:PSS films and reduce the fluidity of the PEDOT:PSS solution. This step is one of the crucial processes for the successful fabrication of organic metasurface absorber. The mask is a chemically etched stainless steel film with a thickness of 0.5 mm. As for spraying process, we employ a miniature commercially available spray gun (HS08DC-S), which is both cost-effective and highly operable, making it suitable for laboratory preparations. In practical applications, industrial spraying equipment would be more appropriate. To achieve uniform films, we employ a sequential horizontal and vertical spraying process, while also optimizing the spraying distance and speed. After the spraying, place the sample on a heating stage for heat treatment at 120 ℃ for 25 minutes, and finally obtain a patterned film with a thickness of approximately 300 nm. Notably, the proposed fabrication process for metasurface absorber is cost effective, efficient, and capable of processing on flexible and irregular surfaces. The final fabricated sample is shown in Fig. 7(a). It can be seen that the sample exhibits good flexibility. We also place the sample on a camouflage pattern and grass [as shown in Fig. 7(b) and 7(c)], demonstrating that the sample possesses good optical transparency, which helps achieve multi-band camouflage purposes.

5. Experiments and Discussion. In order to characterize the absorbing properties of fabricated organic metasurface absorber, a microwave measurement utilizing a vector network analyzer (Keysight, E5063A) is conducted. During the experiment, a pair of horn antennas with operating frequencies up to 18.0 GHz is chosen. We measure the S_{11} and S_{21} under normal incidence, and then calculate the corresponding reflectivity, transmissivity and absorptivity. The measured result is shown in Fig. 8. It can be observed that the transmissivity of the sample is close to 0, and the reflectivity of this sample is lower than 0.1 from 8.1 to 18.0 GHz, indicating that vast majority of electromagnetic waves are absorbed. The absorptivity is approximately greater than 0.9 in the range of 8.1–18.0 GHz, demonstrating the broadband absorber property. Due to the limited working range of the horn antenna used in the experiment, we only measured the performance of the structure up to 18.0 GHz.The experimental results are generally in agreement with simulations. The slight deviation is attributed to preparation conditions.

In practical military applications, multi-band stealth technology (infrared, radar, and visible stealth) has drawn increasing attention. The fabricated metasurface placed on a camouflage pattern is able to achieve stealth in both visible and radar bands [Fig. 7(b)]. Interestingly, we also find that by using organic conductive materials, infrared stealth can be obtained simultaneously. The designed multi-band stealth structure is shown in Fig. 9(a).

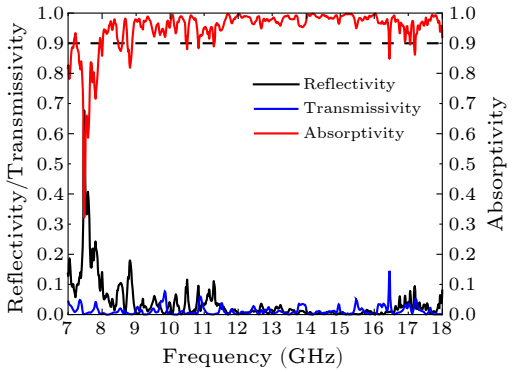

Fig. 8. Measured transmissivity, reflectivity and absorptivity of organic metasurface absorber.

Briefly, a metasurface (infrared stealth layer, ISL) with low infrared emissivity and microwave-transparent property is added to the upper surface of the fabricated absorber. The spacing between ISL and the absorbing structure is about 2 mm, separated by an air layer ($\varepsilon_r \approx 1.0$). The ISL is composed of periodic PEDOT:PSS squares with a side length of 0.8 mm and a spacing of 0.1 mm between adjacent squares. Due to the high reflectivity of PEDOT:PSS films in mid infrared range, it shows low infrared emissivity. The simulated transmission coefficient (S_{21}) of this metasurface is provided in Fig. 9(b), indicating that a good microwave-transparent property can be obtained. The simulated absorptivity of multi-band stealth [Fig. 9(c)] shows that ISL does not affect the broadband absorption. We have fabricated this multi-band stealth structure using a simple method. In the fabrication, place a scraping rod with threads on PEDOT:PSS/PET film and scrape it hard in two mutually perpendicular directions, and then ISL is obtained. As illustrated in Fig. 9(d), the fabricated sample still retains the flexibility and optical transparency. That means this multi-band stealth structure can work in infrared, radar, and visible band.

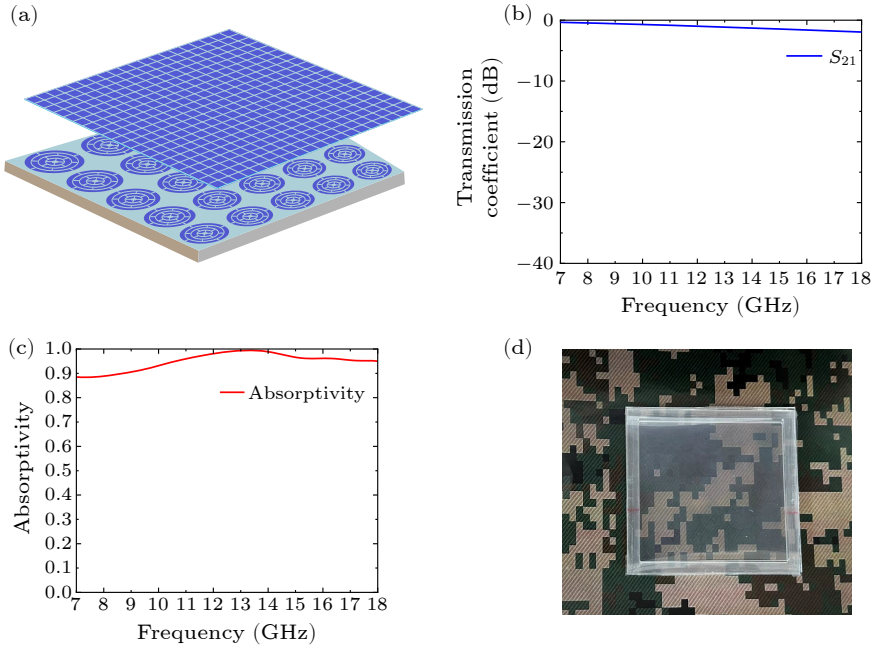

Fig. 9. (a) Schematic of the organic multi-band stealth metasurface. (b) Calculated transmission coefficient of the upper layer. (c) Calculated absorptivity. (d) Photograph of fabricated multi-band stealth metasurface placed on a camouflage pattern.

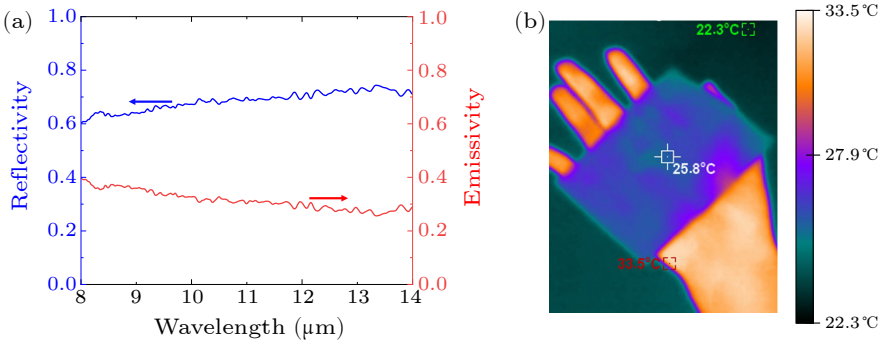

Fig. 10. (a) Measured reflectivity and calculated emissivity of continuous organic conductive film. (b) Infrared thermal image of the proposed structure.

A Fourier transform infrared spectrometer is employed to measure the infrared reflectivity of continuous organic conductive film [Fig. 10(a)]. The wavelength for infrared reflectivity measurement is 8–14 μm, which is often used for detecting individual soldiers. The spectrum reveals that continuous organic conductive film exhibits high infrared reflectivity (R), thus possessing low infrared emissivity ($E = 1 - R$). The average emissivity of continuous organic conductive film is about 0.3, and then the average emissivity of ISL can be calculated as 0.43 due to the filling ratio of organic conductive material is about 0.79. That means the proposed structure has low infrared emissivity, which can be used for infrared stealth. In order to characterize the infrared stealth property of this structure, we use an infrared thermal imager. When the sample is placed on hand palm [Fig. 10(b)], the infrared thermal imager displays that the temperature of the area covered by the structure is significantly lower than that of the hand, indicating its capability of infrared stealth.

To demonstrate that the structure maintains its radar absorbing property, we conduct microwave absorption measurements again. The measured transmission coefficient of the upper structure is shown in Fig. 11(a), indicating that it has good microwave transparency performance. As depicted in Fig. 11(b), the measured reflectivity, transmissivity, and absorptivity reveal that the absorptivity of this structure is approximately greater than 0.9 at around 8.1–18.0 GHz. This confirms that the transparent structure exhibits triple camouflage properties, encompassing infrared, radar, and visible light stealth.

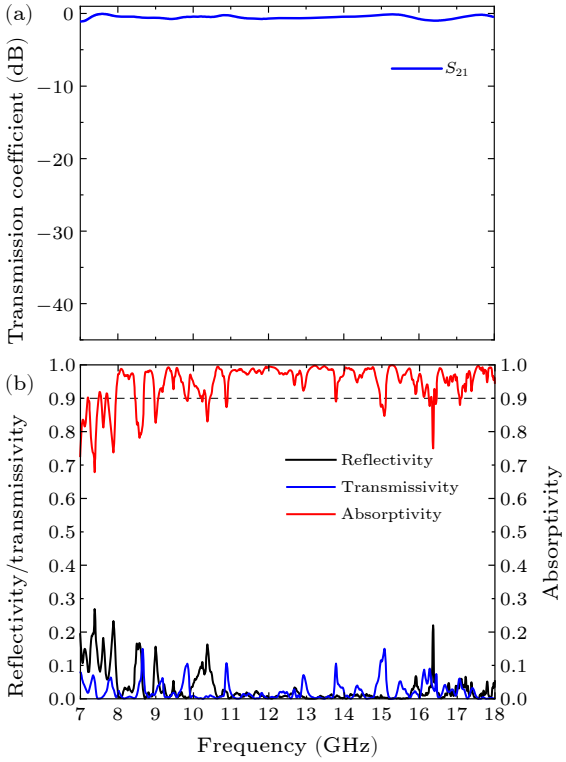

Fig. 11. (a) Measured transmission coefficient of the upper layer. (b) Measured transmissivity, reflectivity and absorptivity of organic multi-band stealth metasurface absorber.

At present, we have investigated the performance of proposed organic metasurface, which can obtain good stealth properties in microwave, infrared, and visible light bands. The relevant innovation points are as follows. Firstly, most of the reported optically transparent metasurfaces are based on inorganic transparent conductive films and we proposed a new way by using an organic metasurface. Secondly, we fould that organic metasurface device has various advantages like foldability, low cost, simple fabrication and can be employed on irregular surfaces.

6. Conclusion. We have demonstrated a flexible, broadband and optically transparent microwave absorber using an organic metasurface. The metasurface absorber is composed of a sandwich structure. It shows a broadband absorption in microwave range. A spraying process was developed to prepare this metasurface absorber. Both simulations and experiments show that this metasurface has broadband microwave absorption and optical transparency. We further found that by using a multi-layer structure, multi-band stealth can be obtained. With the advantages of excellent foldability and low cost, the proposed metasurfaces may have applications in military and wireless communication fields.

Acknowledgements. This work was supported by the National Key R&D Program of China (Grant Nos. 2023YFC3010703, 2020YFB1708800, and 2023YFC3010705).

References

[1] Abdulkarim Y I, Mohanty A, Acharya O P, Appasani B, Khan M S, Mohapatra S K, Muhammadsharif F F, and Dong J 2022 *Front. Phys.* **10** 893791
[2] Zhang C, Yin S, Long C, Dong B W, He D P, and Cheng Q 2021 *Opt. Express* **29** 14078
[3] Ding F, Cui Y X, Ge X C, Jin Y, and He S L 2012 *Appl. Phys. Lett.* **100** 103506
[4] Wang B X, Xu C Y, Duan G Y, Xu W, and Pi F W 2023 *Adv. Funct. Mater.* **33** 2213818
[5] Cui Y, Wang J, Zhu Y, Zhu R C, Sun H T, Xu C L, Wang Z X, Li Y X, Meng Y Y, Wang J F, and Qu S B 2024 *Infrared Phys. Technol.* **141** 105503
[6] Qin Z, Zhang C, Liang Z Z, Meng D J, Shi X Y, and Yang F M 2022 *Adv. Photon Res.* **3** 2100215
[7] Luo M Y, Xie T, Li X, Zheng L, Du T, Zhang Z R, and Yang J B 2024 *Opt. Express* **32** 11221
[8] Wu Y, Tan S J, Zhao Y, Liang L L, Zhou M, and Ji G B 2023 *Prog. Mater. Sci.* **135** 101088
[9] Kwon J H, Hyoung C H, Hwang J H, and Park H H 2021 *Electronics* **10** 237
[10] Namai A, Sakurai S, Nakajima M, Suemoto T, Matsumoto K, Goto M, Sasaki S, and Ohkoshi S 2009 *J. Am. Chem. Soc.* **131** 1170
[11] Karaaslan M, Bağmancı M, Ünal E, Akgol O, and Sabah C 2017 *Opt. Commun.* **392** 31
[12] Yu B Y, Zhao Y J, Chen J Q, Ge Y, and Chen X F 2019 *Int. J. RF. Microw. Comput-Aided. Eng.* **29** e21955
[13] Mohammed S A, Kamil Albadri R A, and Al-Badri K S L 2023 *Heliyon* **9** e19466
[14] Duan G, Schalch J, Zhao X, Zhang J, Averitt R D, and Zhang X 2018 *Phys. Rev. B.* **97** 035128
[15] Zhang J, Li Z F, Shao L D, and Zhu W R 2021 *Carbon* **176** 374

[16] Jeong H, Tentzeris M M, and Lim S 2019 *Materials* **12** 3406
[17] Yang C, Chang H C, Xiao L, and Qu Y C 2022 *Opt. Mater.* **131** 112464
[18] Hu D W, Cao J, Li W, Zhang C, Wu T L, Li Q F, Chen Z H, Wang Y L, and Guan J G 2017 *Adv. Opt. Mater.* **5** 1700109
[19] Gao G, Huang Y, Zeng S Q, Li K, Zhang Y M, and Zhu J Q 2024 *Appl. Surf. Sci.* **658** 159830
[20] Cui Y N, Wang J, Sun H T, Zhu Y, Zhu R C, Liu T H, Wang X F, Xu C L, Wang J F, Qu S B 2024 *Adv. Opt. Mater.* **12** 2301712
[21] Park S, Shin G Y, Kim H, Kim Y W, and Yoon I 2021 *Appl. Sci.* **11** 9315
[22] Ge J C, Yan W B, Zhang H Y, Li L Y, Wang D X, Xu K D, and Hong T 2024 *Opt. Express* **32** 32002
[23] Zhang C, Cheng Q, Yang J, Zhao J, and Cui T J 2017 *Appl. Phys. Lett.* **110** 143511
[24] Zhao J, Zhang C, Cheng Q, Yang J, and Cui T J 2018 *Appl. Phys. Lett.* **112** 073504
[25] Lai S F, Wu Y H, Zhu X B, Gu W H, and Wu W 2017 *IEEE. Photonics J.* **9** 1
[26] Xu J, Fan Y C, Su X P, Guo J, Zhu J X, Fu Q H, and Zhang F L 2021 *Opt. Mater.* **113** 110852
[27] Zheng Y L, Chen K, Jiang T, Zhao J M, and Feng Y J 2019 *J. Phys. D. Appl. Phys.* **52** 335101
[28] Bai X L, Mei Z L, Zhang J W, Xu W B, Lin W J, and Niu T M 2024 *IEEE. Antennas. Wirel. Propag. Lett.* **23** 1543
[29] Ma Y, Shi L H, Wang J B, Zhu L Y, Ran Y Z, Liu Y C, and Li J 2021 *J. Mater. Sci. Mater. Electron* **32** 2001
[30] Liu R, Zhang B Z, Duan J P, Dong L, Yu J, and Zhang Z H 2020 *Mater. Res. Express* **7** 045803
[31] Chen P, Kong X L, Han J F, Wang W H, Han K, Ma H Y, Zhao L, and Shen X P 2021 *Chin. Phys. Lett.* **38** 027801
[32] Gu C, Qu S B, Pei Z B, Zhou H, Zhou X, Bai P, and Lin B Q 2010 *Chin. Phys. Lett.* **27** 117802
[33] Dong Y F, Yu D W, Li G C, Cao Y L, Ruan Y D, and Lin M T 2021 *Crystals* **11** 1583
[34] Okano Y, Ogino S, and Ishikawa K 2012 *IEEE. Trans. Microw. Theory. Tech.* **60** 2456
[35] Shen Y, Zhang J Q, Sui S, Jia Y X, Pang Y Q, Wang J F, Ma H, and Qu S B 2018 *J. Phys. D. Appl. Phys.* **51** 485301
[36] Gao Z Q, Xu C L, Tian X X, Wang J F, Zhang H H, Qu S B, and Fan Q 2021 *Opt. Commun.* **500** 127327
[37] Li M L, Muneer B, Yi Z X, and Zhu Q 2018 *Adv. Opt. Mater.* **6** 1701238
[38] Huang Y, Zhu Y N, Qin B, Zhou Y W, Qin R, Ghosh P, Qiu M, and Li Q 2022 *Nanophotonics* **11** 3613
[39] Zhu H Z, Li Q, Tao C N, Hong Y, Xu Z Q, Shen W D, Kaur S, Ghosh P, and Qiu M 2021 *Nat. Commun.* **12** 1805
[40] Xu C L, Wang B K, Yan M B, Pang Y Q, Wang W J, Meng Y Y, Wang J F, and Qu S B 2020 *J. Phys. D. Appl. Phys.* **53** 135109
[41] Li H Y, Yuan H, Costa F, Cao Q S, Wu W, and Monorchio A 2021 *Opt. Express* **29** 42863
[42] Han K, Shim H B, and Hahn J W 2022 *Adv. Photon Res.* **4** 2200009
[43] Meng Z, Tian C H, Xu C L, Wang J F, Huang S N, Li X H, Yang B Y, Fan Q, and Qu S B 2020 *Infrared Phys. Technol.* **110** 103469
[44] Zhong S M, Jiang W, Xu P P, Liu T J, Huang J F, and Ma Y G 2017 *Appl. Phys. Lett.* **110** 063502
[45] Wen K H, Han T C, Lu H P, Luo W, Zhang L B, Chen H Y, Liang D F, and Deng L J 2021 *Opt. Express* **29** 8872
[46] Liu Y N, Weng X L, Zhang P, Li W X, Gong Y, Zhang L, Han T C, Zhou P H, and Deng L J 2021 *Chin. Phys. Lett.* **38** 034201
[47] Huseynova G, Hyun Kim Y, Lee J H, and Lee J 2020 *J. Inf. Disp.* **21** 71
[48] Smith D R, Vier D C, Koschny T, and Soukoulis C M 2005 *Phys. Rev. E* **71** 036617
[49] Chen X D, Grzegorczyk T M, Wu B I, Pacheco J, and Kong J A 2004 *Phys. Rev. E* **70** 016608